Journal of Neuroscience Methods 336 (2020) 108634

Contents lists available at ScienceDirect

Journal of Neuroscience Methods

journal homepage: www.elsevier.com/locate/jneumeth

Invited review

Acute *in vivo* testing of a polymer cuff electrode with integrated microfluidic channels for stimulation, recording, and drug delivery on rat sciatic nerve

Sahar Elyahoodayan[a], Christopher Larson[a], Angelica M. Cobo[a], Ellis Meng[a,b], Dong Song[a,c,*]

[a] Department of Biomedical Engineering, University of Southern California, Los Angeles, CA 90089, USA
[b] Department of Electrical and Computer Engineering, University of Southern California, Los Angeles, CA, 90089, USA
[c] Neuroscience Graduate Program, University of Southern California, Los Angeles, CA, 90089, USA

ARTICLE INFO

Keywords:
Electrophysiology
Peripheral nerve
Cuff electrode
Drug delivery

ABSTRACT

Background: Extraneural cuffs are among the least invasive peripheral nerve interfaces as they remain outside the nerve. However, compared with more invasive interfaces, these electrodes may suffer from lower selectivity and sensitivity since the targeted nerve fibers are more distanced from the electrodes.
New Method: A lyse-and-attract cuff electrode (LACE) was enabled by microfabrication and developed to improve selectivity and sensitivity while maintaining a cuff format. Its engineering design was described in previous work. LACE is a hybrid cuff that integrates both microelectrodes and microfluidic channels. The ultimate goal is to increase fascicular selectivity and sensitivity by focal delivery *via* the microchannels of (1) lysing agent to remove connective tissue separating electrodes from nerve fibers, and (2) neurotrophic factors to promote axonal sprouting of the exposed nerve fibers into microfluidic channels where electrodes are embedded. Here, we focus on demonstrating *in vivo* function of microfluidics and microelectrodes in an acute preparation in which we evaluate the ability to focally remove connective tissue and record and stimulate with microchannel-embedded microelectrodes neural activity in rat sciatic nerves.
Comparison with existing methods: While extraneural interfaces prioritize nerve health and intraneural interfaces prioritize functionality, LACE represents a new extraneural approach which could potentially excel at both aims.
Results: Surgical implantation demonstrate preservation of LACE function following careful and minimal handling. *In vivo* electrical evaluation demonstrates the ability of microelectrodes placed within microfluidic channels to successfully stimulate and record compound action potentials from rat sciatic nerve. Furthermore, collagen-rich epineurium was focally removed following infusion of collagenase *via* microchannels and confirmed *via* microscopy.
Conclusion: The feasibility of using a cuff having integrated microelectrodes and microfluidics to stimulate, record, and deliver drug to focally lyse away the epineurium layer was demonstrated in acute experiments on rat sciatic nerve.

1. Introduction

Peripheral nerve interfaces aim to provide therapies for various diseases or restoration of lost functions through their interactions with the peripheral nervous system. For example, electrical stimulation of the peripheral nerve *i.e.* sciatic, ulnar, and occipital nerve have been used to treat chronic pain (Sun and Morrell, 2014), (Picaza et al., 1977). Therapeutic modulation of organ functions through vagus nerve stimulation (VNS) has demonstrated success in controlling blood pressure (Plachta et al., 2014), reducing body fat (Banni et al., 2012), suppressing epileptic seizures (Zabara, 1985), and treating arthritis (Giagka and Serdijn, 2018), (Koopman et al., 2016). Furthermore, bidirectional recording and stimulation from peripheral nerves has become an important approach for achieving closed-loop control of neural prostheses such as robotic hands (Schultz and Kuiken, 2011)–(Tan et al., 2015) or a limb after spinal cord injury (Russell et al., 2019), (del Valle and Navarro, 2013). In all applications of peripheral nerve interfaces, selective recording and stimulation of nerve fibers within a nerve bundle is highly desired so that targeted neural effects can be achieved while undesired off-target effects are avoided. For example, motor control requires recording and translating neural commands from efferent fibers within the nerve, while stimulating afferent fibers to send sensory

* Corresponding author at: University of Southern California, 403 Hedco Neuroscience Building, Los Angeles, CA, 90089, USA.
E-mail addresses: elyahood@usc.edu (S. Elyahoodayan), larsonce@usc.edu (C. Larson), acobo001@gmail.com (A.M. Cobo), ellis.meng@usc.edu (E. Meng), dsong@usc.edu (D. Song).

https://doi.org/10.1016/j.jneumeth.2020.108634
Received 3 December 2019; Received in revised form 11 February 2020; Accepted 11 February 2020
Available online 14 February 2020

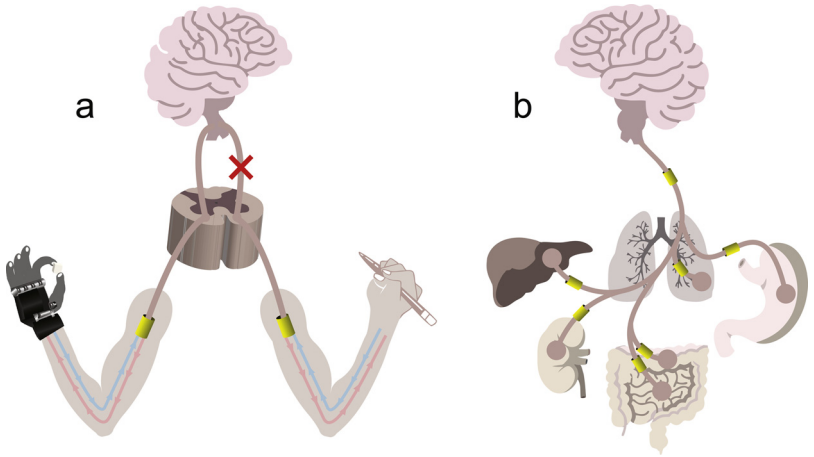

Fig. 1. Peripheral nerve interfaces can be used for a) closed-loop control of prostheses or limbs after spinal cord injury, and b) modulation of various organs.

feedback to the user. Furthermore, organ modulation *via* nerve stimulation, as in bioelectronic medicine, requires selective targeting of the specific fibers within a nerve trunk that innervate the organ of interest (Fig. 1).

Extraneural cuff electrodes provide a minimally invasive method to interface with the peripheral nerve as they wrap gently around the nerve and stimulate or record from multiple nerve fibers with non-penetrating surface electrodes. They enclose the circumference of the nerve with an insulative material to restrict ionic currents. Metal electrodes on the inner wall of the cuff enable stimulation and recording of the encircled nerve fibers (Grill and Mortimer, 1996), (Marks and Loeb, 1976). More recent cuff electrodes take advantage of microfabrication techniques and are made from thin-film polymers and metals. They consist of insulated thin-film metal traces, exposed electrode sites and integrated interconnects that allow external connection (Caravaca et al., 2017), (Rodríguez et al., 2000). Ideally, the cuff diameter can be adjustable to fit nerves of varying sizes, thereby allowing surgical flexibility and better integration of the cuff with the nerve (Loeb and Peck, 1996), (Elyahoodayan et al., 2018).

Cuff electrodes induce minimal immune response when properly installed (Navarro et al., 2005). However, electrodes on the surface of the cuff are separated from nerve fibers by the epineurium and perineurium and therefore suffer from lack of selectivity and sensitivity (Loeb and Peck, 1996), (Kang et al., 2015), (Hoffer and Kallesøe, 2001). A variety of strategies have been investigated to improve selectivity and sensitivity (Larson and Meng, 2019), including extraneural cuffs which reshape the nerve (Leventhal and Durand, 2003), (Schiefer et al., 2010), (Leventhal et al., 2006), (Caparso et al., 2009) and intrafascicular electrodes which penetrate the nerve trunk (Lawrence et al., 2002), (Badia et al., 2011). Such approaches have varying degrees of success in improving device functionality while maintaining long-term performance and nerve health. The latter penetrating approach is highly invasive and breaches the integrity of the nerve. To our knowledge, non-surgical methods to focally remove epineurium and perineurium have not been explored in conjunction with cuff electrodes.

To provide a means to evaluate such an approach towards achieving fascicular selectivity and sensitivity, we developed a novel hybrid, multi-functional cuff electrode (Cobo et al., 2019). The design consists of a microfabricated thin-film polymer cuff with electrodes for recording and stimulation, and microfluidic channels to deliver drugs focally. The microfluidic channels terminate in a well-defined outlet and allow focal drug delivery of a chemical lysing agent to non-surgically remove connective tissue and thereby minimize the distance between the electrodes and nerve fibers without introducing mechanical trauma to the nerve. The resulting "window" provides greater access to the underlying nerve fibers for electrodes on the cuff. This could possibly be enhanced further by delivery of neurotrophic factors in order to attract axonal sprouting towards the electrodes within the channels. Reflective of this design concept, the device has been termed the *lyse-and-attract cuff electrode* (LACE) (Cobo et al., 2019).

The engineering design, fabrication, packaging, electrical characterization and fluidic performance of LACE on a benchtop set-up were demonstrated in a previous study (Cobo et al., 2019). In this paper, the implantation procedure and a systematic evaluation of the LACE's capability to acutely record, stimulate, and deliver lysing agent to rat sciatic nerves *in vivo* is described. LACE was implanted in an acute preparation. Then evoked neural response to electrical stimulation with varying magnitudes were recorded, validated, and characterized. Next, nerve stimulation with electrochemically reversable stimulation pulses to evoke muscle activation was performed. Finally, collagen fibers of the epineurium layer were focally removed by delivery of collagenase *via* the microfluidic channels. The acute effects of focal delivery were evaluated using histology and label-free two-photon imaging and these results correlated to confirm focal lysing of the epineurium on the nerve's surface. The findings indicate the electrodes' recording and stimulation capabilities from within the microfluidic channels. They further demonstrate the capability of LACE to perform chemical manipulation of the electrode-tissue interface.

2. Experimental methods

2.1. Design and fabrication

LACE (Fig. 2) is a flexible thin-film polymer device featuring metal electrodes for recording and stimulation, microfluidic channels for drug delivery, and an adjustable locking mechanism for precise fitting

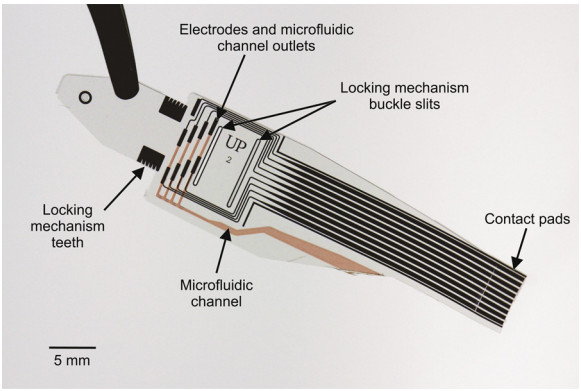

Fig. 2. Fabricated Parylene C cuff electrode with integrated microfluidic channels. A red photoresist layer is shown in the channels for visibility.

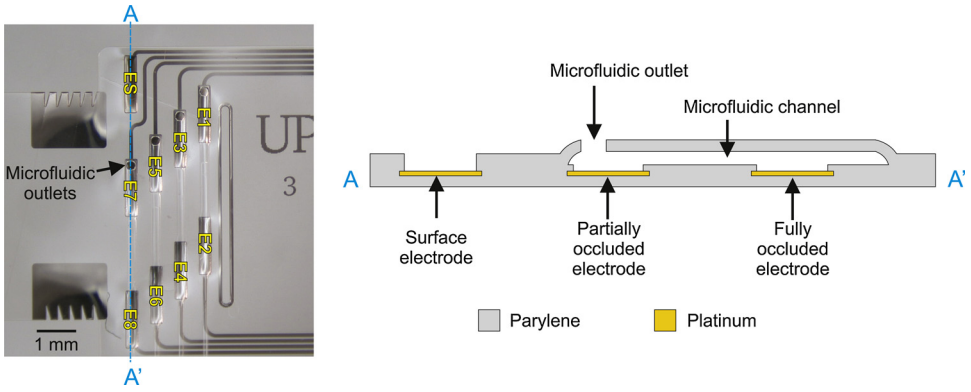

Fig. 3. Magnified view of the microfluidic outlets and the electrode arrangement (left) and illustrated cross section of one channel and its electrodes (right). Electrodes E1, E3, E5, and E7 are partially occluded by the microfluidic channels with the outlets directly above the electrodes. Electrodes E2, E4, E6, and E8 are fully occluded by the channel (not used in experiments described in this paper). The surface electrode (ES) is fully exposed.

around the nerve. It is fabricated from Parylene C using surface micromachining techniques on a temporary silicon wafer carrier. Four microfluidic channels are spaced 350 µm apart on the circumference of the nerve, each with a 20 µm H × 250 µm W cross-section and 200 µm-diameter outlets. The electrode layout is shown in Fig. 3. Eight metal electrodes (300 µm × 1500 µm) made from 200 nm-thick platinum are arranged as a bipolar pair inside each microfluidic channel. One electrode of each pair is directly beneath the microfluidic outlet while the second is approximately 4 mm away from the outlet. A ninth electrode of the same dimensions is located outside the channels (the surface electrode). The locking mechanism consists of a tab which is led by suture through a slit which catches on a set of ratchet-like teeth. The series of locking teeth allow for adjustable sizing to fit nerves of 1.1–1.5 mm diameter in 0.1 mm increments.

2.2. Surgical technique

Surgery was performed on male Wistar rats (> 9 weeks old, 300 – 400 g). All animal experiments were approved by the Institutional Animal Care and Use Committee (IACUC) and the Department of Animal Resources of the University of Sothern California (DAR, USC). Animals were anesthetized with 0.2 mL/100 g of ketamine and xylazine. Anesthesia was maintained throughout the surgical procedure by inhalation of a mixture of oxygen and isoflurane.

A midsagittal incision was made at the right thigh. Junction between muscles was identified and pulled apart by blunt dissection. The sciatic nerve was exposed; blood was rinsed off using 1 × phosphate-buffered saline (PBS). LACE was then implanted around the right sciatic nerve with a 4.0 suture needle. The suture was knotted at one end and the needle was threaded through a hole in the electrode tab (Fig. 4a). After LACE was guided under and then around the nerve, the suture needle was passed through the first slit and locked in place by pulling on the suture at one end and the FFC cable connected to the electrode at the opposite end (Fig. 4b). This technique allows for easy implantation with minimal to no damage to the electrode or tissue.

2.3. Recording set-up

The connection scheme for the electrophysiological recording setup is illustrated in Fig. 5a. Evoked compound action potentials (CAP), a summation of action potentials generated by multiple fibers, were recorded differentially between the surface electrode and E7. A large platinum wire was placed on the exposed muscle of the animal near the incision as ground. The recording amplifier (A–M systems, model 1700) was set to 80 dB gain with a 10 Hz – 10 kHz band pass filter. All signals were digitized and recorded with a recording system (Digidata 1322A, Molecular Devices) and data were saved with pClamps9 software (Molecular Devices) using a 100 kHz sampling frequency.

Bipolar needle electrodes were inserted into the nerve 20 mm from the recording site and were connected to an external stimulator (Multichannel Systems STG4000). Biphasic, cathodic-first pulses with a fixed duration of 200 µs (Cogan, 2008), and amplitudes of 100–700 µA in steps of 50 µA were delivered.

After normal CAPs were recorded, a negative control experiment was performed to verify the neural nature of the recorded signals. Lidocaine was applied to the sciatic nerve distal from the stimulation site. Lidocaine is a local anesthetic that prevents the generation and conduction of action potentials in a nerve by binding to and blocking fast inactivation voltage-gated Na + channels (Vedantham and Cannon, 1999). Therefore, application of lidocaine would abolish neural activity to demonstrate that the recorded data was indeed neural activity, not noise or artifact from stimulation.

The nerve was then stimulated while the leg muscle was observed for twitching. Twenty minutes after application of lidocaine, no muscle twitch in response to nerve stimulation was observed. Nerve recordings were then performed with the same stimulation paradigm using LACE (Fig. 5b). Subsequently, while nerve conduction was still blocked by lidocaine, the leg muscle was stimulated directly using needle electrodes, producing a twitch. While directly stimulating the muscle, recording from the nerve was performed to verify whether EMG activity contaminated the previous CAP recordings (Fig. 5c).

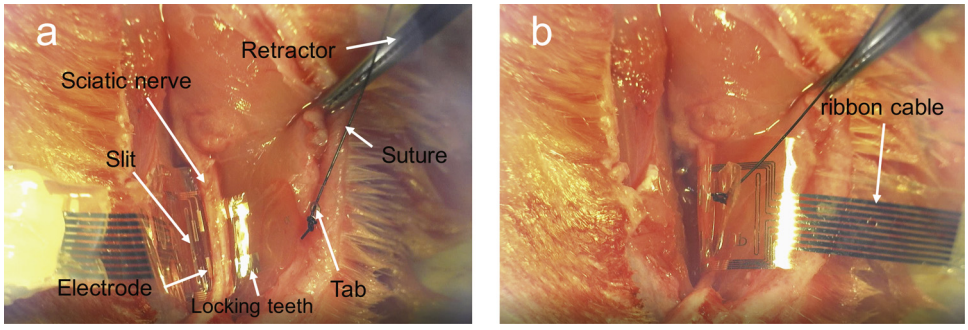

Fig. 4. a) LACE threaded underneath sciatic nerve. b) LACE locked around the sciatic nerve.

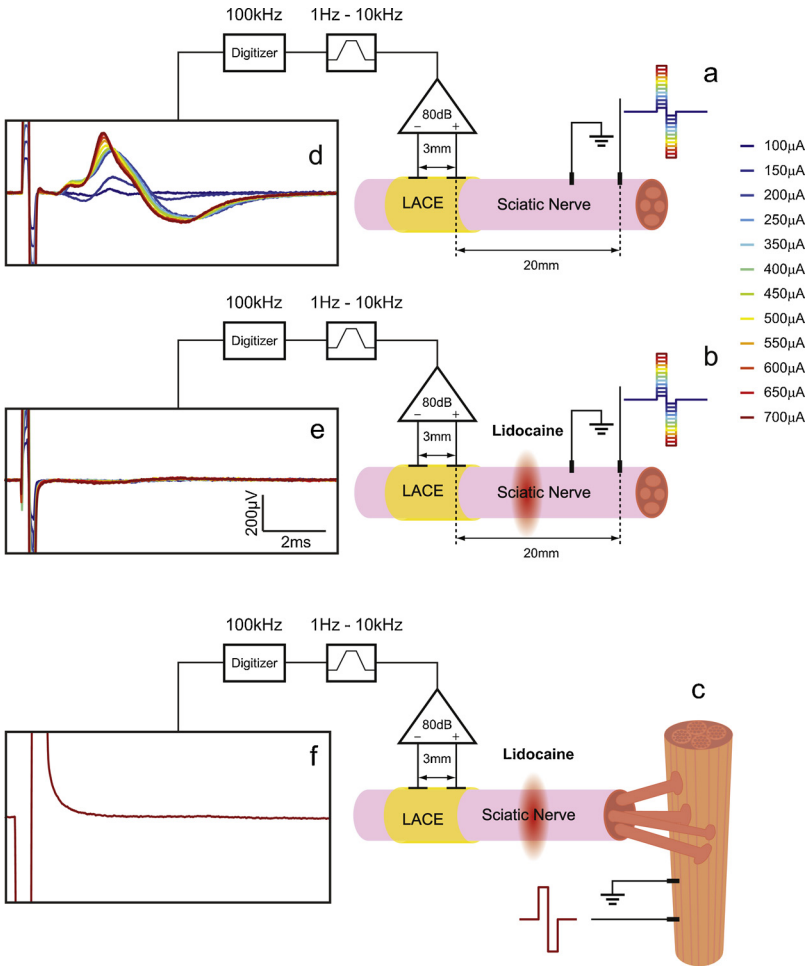

Fig. 5. Acute *in vivo* recording setup is shown on the right of each panel, and the corresponding recordings from LACE are shown on the left. a) LACE was used to record neural activities from the nerve. E7 was used as the working electrode and SE was used as the reference electrode. Stimulation pulses were applied to the nerve 20 mm from the recording site using needle electrodes. The stimulation pulses were charge-balanced anodic-first biphasic pulses with a fixed duration of 200 µs, and pulse amplitudes ranging from 100 µA to 700 µA in steps of 50 µA. The recording amplifier was set to a gain of 80 dB, with 10 Hz-10 kHz band pass filter. b) Lidocaine was applied to the nerve distal from the stimulation electrodes and (a) was repeated. c) Lidocaine was again applied to the nerve, the leg muscle was stimulated at 700 µA, and activity was recorded from the nerve using LACE. d) CAPs elicited with stimulations of varying amplitude were recorded using LACE. e) and f) are verification of recorded nerve response. e) Application of lidocaine to the nerve abolished neural responses while stimulation artifacts were unchanged. f) EMG artifacts are absent during direct muscle stimulation.

2.4. Stimulation set-up

Fig. 7a illustrates the stimulation set-up. The rat sciatic nerve is composed of tibial and peroneal divisions which innervate the thigh, leg and foot muscle. For stimulation testing, the stimulus was applied to E5 as the working electrode and surface electrode as the return. Motor responses were monitored from compound muscle potentials of the extensor digitorum longus muscle recorded by bipolar needle electrodes. The bipolar recording electrodes were positioned to record differentially along the longitudinal direction of the muscle fibers. Again, a negative control was performed by applying lidocaine to the nerve and recording responses from the same muscle (Fig. 7b).

2.5. Drug delivery

Before implantation, the microfluidic channels were primed with collagenase as described previously (Cobo et al., 2019). Once LACE was implanted, collagenase was infused at 0.1 µl/min for 10 min. This flow rate was previously determined by benchtop experiments with dye on a nerve phantom, which resulted in localized delivery with no diffusion (Cobo et al., 2019). The reaction time of collagenase to lyse the epineurium is approximately one hour (Rydevik et al., 1985). Thus, one hour after delivery, the nerve was excised, and the rat was euthanized with compressed carbon dioxide gas. The tissue was fixed by immersion in 10 % formalin solution for an hour in 4 °C to preserve morphology. It was then transferred to 30 % sucrose solution to dehydrate it overnight. Two-photon (2 P) second harmonic generation (SHG) microscopy was used to examine the nerve structure. SHG does not require labeling with molecular probes and is thus a non-destructive technique to image tissue anatomy (Vijayaraghavan et al., 2014). Collagen is a non-centrosymmetric molecule emitting exactly half of the wavelength of the excitation wavelength (Zoumi et al., 2002), (Campagnola et al., 2002) and provides sufficient signal for SHG imaging. Since the peripheral nerve is rich in collagen, SHG is a suitable technique to image collagen fibrils at high resolution (Sinclair et al., 2012).

The tissue was whole mounted in 1% clear agarose gel. SHG imaging was carried out on a commercial scanning Zeiss LSM510NLO two-photon microscope. The excitation wavelength was set to 900 nm and SHG signal was collected using a 420 − 460 nm bandpass filter. All images were acquired with a 25x/1.05 numerical aperture water immersion lens. The nerve was tile-scanned with a field of view of 600 × 600 µm. The axial and lateral resolution was set to 10 µm.

After 2 P-SHG imaging, agarose was removed and the tissue was mounted in optimal cutting temperature (OCT) compound and frozen at − 80 °C. It was then sectioned at 30 µm on a cryostat and treated by H&E staining to observe the quality and location of lysing activity. Stained samples were imaged using a DM2500 microscope and a DFC450 digital camera (Leica Microsystem, Cambridge, UK). The lysed regions were measured by Leica Application Suite Version 4.

3. Results

3.1. Fabrication results

The electrodes were fabricated, packaged, and characterized as described in (Cobo et al., 2019). Benchtop tests verified function of the microfluidic channels and locking mechanism. Cyclic voltammetry (CV) was performed in 0.05 M H_2SO_4 to clean the electrodes of any residues

that may remain after fabrication. CV and electrochemical impedance spectroscopy (EIS) were then performed in phosphate buffered saline (PBS) to assess stimulation characteristics. From integration of the CV with a scan rate of 250 mV/s, cathodal charge storage capacity of the platinum electrodes was 1.1 ± 0.1 mC/cm2 (mean ± SE, n = 4) and impedance at 1 kHz was 1.8 ± 0.11kΩ (n = 6). Devices were disinfected by soaking for 15 min in isopropanol.

3.2. Acute recording test

Evoked CAP responses were recorded from rat sciatic nerves using LACE (n = 3). Fig. 5d shows a representative example of overlaid CAP responses elicited by stimuli with varying amplitudes. The CAP responses increase in magnitude with the stimulus magnitude, indicating that stronger stimuli recruit more nerve fibers which constructively add to produce a larger CAP response at the recording site. Since the recording is bipolar, there are two phases to the CAP activity: a positive followed by a negative phase. This arises from the connection scheme, having the recording electrode proximal to the stimulation electrode connected to the non-inverting input of the differential amplifier and the distal electrode connected to the inverting input. The temporal dispersion of the CAP waveform is due to variability in conduction velocity across nerve fibers (Liang et al., 1991), (Maynard et al., 1997). Larger myelinated axons have faster conduction velocity due to smaller axial resistance. Also, large diameter axons have lower threshold to extracellular current due to smaller axial resistance, allowing more efficient passage of longitudinal extracellular current (Lloyd et al., 1946), (Huxley and Stämpeli, 1949).

Fig. 5e verifies the neural nature of the recorded signals. After application of lidocaine, elimination of responses following stimulation confirmed that the recorded signals shown in Fig. 8a were indeed neural. Furthermore, the leg muscle was stimulated with a needle electrode to evoke EMG activity. Fig. 5f demonstrates that, after application of lidocaine to the nerve proximal from the neuromuscular junction, only stimulation artifacts

were recorded by LACE, while no response was observed. This result further verifies that the signals shown in Fig. 8a were not EMG or contaminated by EMG.

Each neural response to its respective stimulus was rectified and integrated. The mean over three trials for each response was computed and the obtained values were normalized by the maxima and plotted *versus* the stimulus magnitude (Fig. 6a). Here, the threshold stimulation current for eliciting CAP was 100 µA. The plot demonstrates a steep slope for stimuli below 200 µA and a very shallow slope for stimuli greater than 200 µA suggesting gradual saturation of number of recruited fibers above 200 µA.

Fig. 6b illustrates the latency-to-onset of CAP *versus* the stimulation amplitude. Since large diameter fibers are recruited first and have faster conduction velocity than small diameter fibers, this plot is relatively flat. At a distance of 20 mm between stimulation and recording electrodes, the latencies provide an approximation of conduction velocities of 16 − 21 m/s. Conduction velocities are consistent with values previously reported in rat sciatic nerve experiments (Yu et al., 2014), (Xue et al., 2015).

3.3. Acute stimulation test

The stimulation tests after acute implantation verified that LACE can deliver enough charge to the nerve to cause muscle contractions. Fig. 7 c shows an example of recordings from extensor digitorum longus muscle with increasing stimulation intensity. The recording is from multiple motor unit action potentials, adding up temporally and spatially to generate complex waveforms. The maximum stimulus applied across the electrode is 0.04 µC. This is well below the charge storage capacitance of LACE at ~4.5 µC, ensuring delivery of electrochemically reversable stimulation pulses.

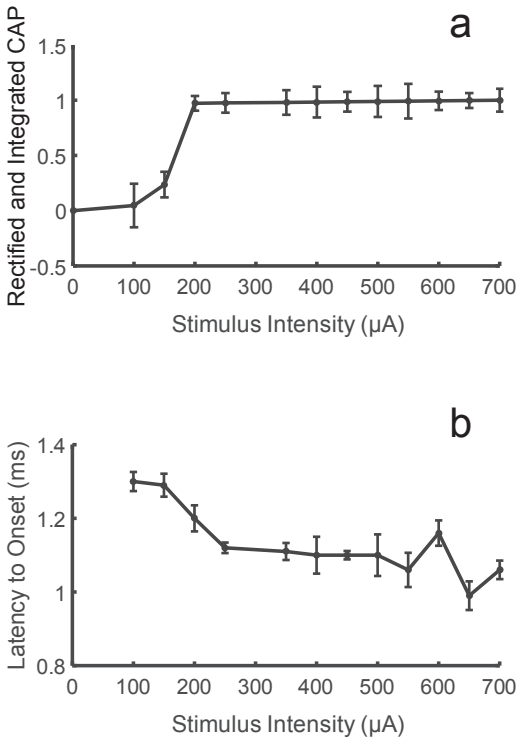

Fig. 6. Recruitment curve of sciatic nerve fibers. Error bars are standard error mean values from three rats. a) Rectified and integrated values of each CAP activity following stimulation. The integrated CAPs are normalized by the maxima and plotted *versus* the stimulus intensity. b) Latency to onset *versus* the stimulus intensity.

As before, Fig. 7d is a verification of recorded neural activities. After application of lidocaine, the absence of any activity following stimulation confirms that the recorded signals are biological.

3.4. Drug delivery

A rendering of LACE installed on a nerve is illustrated in Fig. 8 a. Histological results demonstrated effects of collagenase treatment on the morphology of sciatic nerves. Tissue closest to the microfluidic channel openings demonstrated obvious disruption of epineurium (Fig. 8b) whereas tissue further away from the microfluidic channel openings was unaffected (Fig. 8C). The lysed region was ~300 µm of the nerve's perimeter, which is comparable to the diameter of the microfluidic channel outlet (200 µm). This result suggests that the chosen flow rate and duration produced a focal distribution of collagenase effects on the surface of the nerve with ~50 µm diffusion beyond the edge of the outlet.

Tile-scanned SHG images were acquired using a 900 nm excitation wavelength. The acquired scans were then z-stacked in Imaris image analysis software to construct a 3D rendering (Fig. 9a). The green regions indicate emission from collagen fibers, while diminished signal is representative of collagen absence. A dark circular region with a diameter of 290 nm, enlarged in Fig. 9b, showed a clear, focal removal of collagen. Again, this shape and dimension is comparable to the outlet of the LACE microfluidic channel (Fig. 9c) and agrees with the lysed region found in transverse histological sections.

4. Discussion

In this study, we developed the surgical technique to implant LACE in rat sciatic nerves with minimal handling of the device and the tissue. The adjustable locking mechanism allowed for simple adjustment of the LACE around nerves of various diameters. After implantation, device

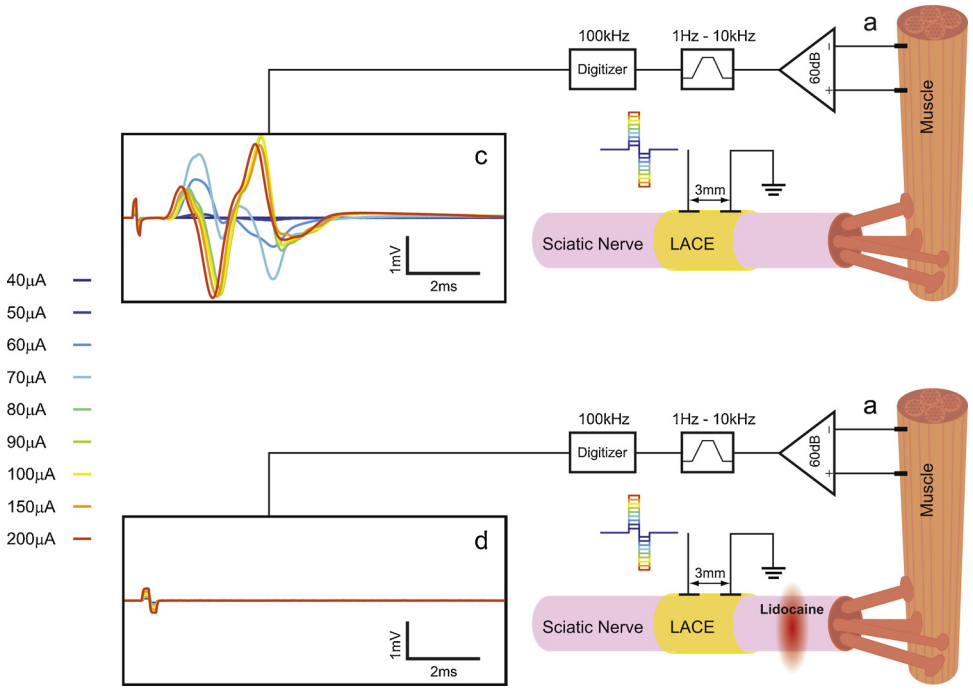

Fig. 7. Acute *in vivo* stimulation setup is shown on the right panel, and corresponding recorded evoked EMG shown on the left panel. a) E5 was used as the working stimulation electrode and SE was used as the reference. Anodic-first stimulation pulses set to a fixed pulse duration of 200 μs and amplitudes ranging from 40 μA to 200 μA were applied. EMG was recorded bipolarly using needle electrodes in the extensor digitorum longus muscle in the rat's right hind leg. The recording amplifier was set to a gain of 60 dB with 10 Hz-10 kHz band pass filter. b) Lidocaine was applied proximal from the neuromuscular junction and (a) was repeated. c) EMG activity recorded following nerve stimulation. d) Verification of the recorded muscle response. Application of lidocaine to the nerve abolished EMG response while the stimulus artifact was unchanged.

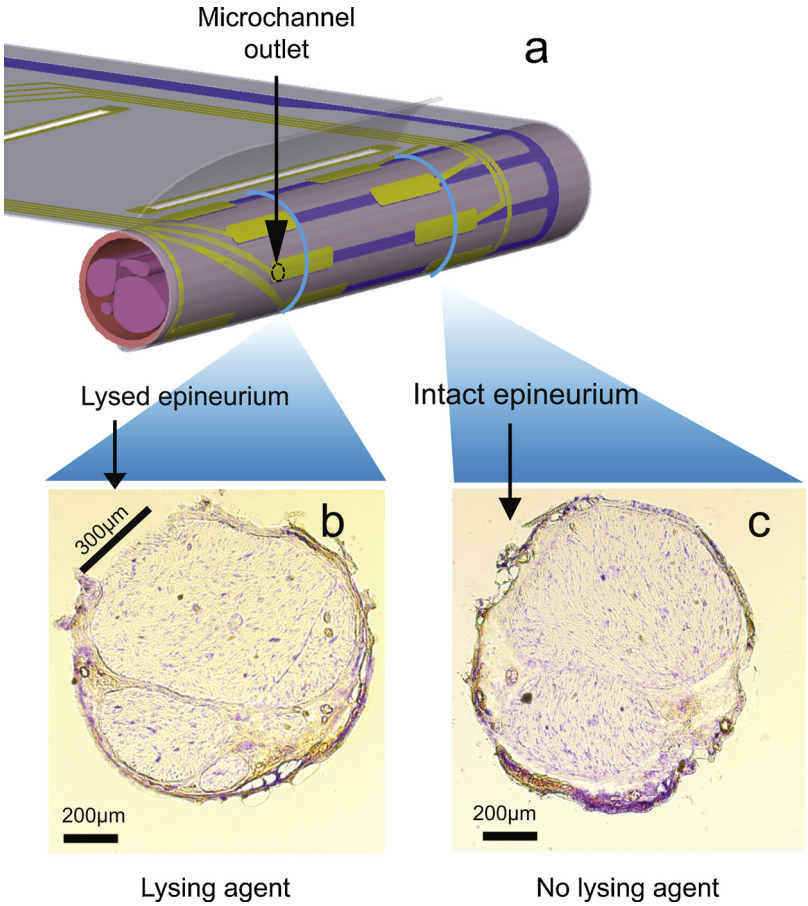

Fig. 8. Demonstration of the effect of lysing agent on exterior connective tissue of the nerve. a) Rendering of the LACE installed on the nerve. b) Histology slides after delivery of collagenase show that it effectively disrupted the epineurium near the microchannel outlet. c) Away from the outlets, the epineurium was intact.

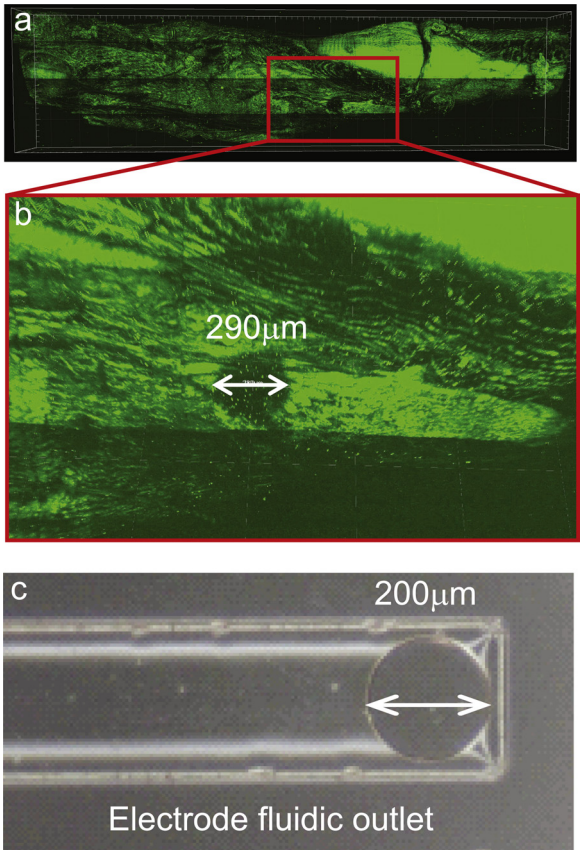

Fig. 9. a) 2 P-SHG images of whole mount nerve tissue with excitation wavelength of 900 nm. b) A circular dark region, magnified, indicates absence of collagen fibers. Comparison of the dimensions of the dark region (290 μm diameter) with c) the microchannel outlet (200 μm diameter) demonstrates focal delivery.

integrity and function were maintained. This enabled demonstration of LACE's capability to record neural activity from rat sciatic nerves, and to deliver charge to stimulate the nerve and evoke muscle response. The recorded signals were confirmed to have neural origin by comparing evoked potentials before and after application of lidocaine to the nerve. Leg muscle innervated by the implanted nerve was also stimulated to confirm absence of EMG artifact in the recorded nerve signals. The bipolar recording configuration, using an electrode partially inside the microfluidic channel and a surface electrode, obtained neural activities in response to increasing stimulation pulses similar to recordings previously reported using the same set-up (Yu et al., 2014), (Xue et al., 2015). Furthermore, stimulation of the nerve through LACE was successfully demonstrated in muscle activity recorded with needle electrodes in the rat hind leg.

Although cuff electrodes have been used successfully in animals and humans (Graczyk et al., 2016), (Guiraud et al., 2016), there has been limited success in recording nerve fibers with high sensitivity and stimulating them with high selectivity. Some peripheral interfaces achieve higher acute performance by sacrificing the long-term health of the nerve. Microscale drug delivery, as demonstrated using the LACE, may offer an alternative strategy. We demonstrated the capability of LACE to deliver controlled boluses of drug focally to biochemically manipulate the electrode-tissue interface. Histological analysis and 2 P-SHG imaging suggest that collagenase lysed the epineurium layer focally with minimal diffusion from the microfluidic outlet. This is in comparison to previous work (Rydevik et al., 1985), where an uncontrolled large bolus of 1 ml of collagenase was applied around the tibial nerve to study the effect of collagenase on nerve tissue.

Following the focal lysing of epineurium which has now been demonstrated, LACE provides an ideal setup to potentially take advantage of the phenomenon of collateral sprouting of nerve fibers. Application of neurotrophic factors, such as NGF and methylcobalamin, has been shown to enhance collateral sprouting from an intact nerve (McCallister et al., 2001). Collateral sprouting of nerve fibers following microsurgical removal of the epineurium layer from the nerve has been demonstrated in both sensory and motor fibers (Šámal et al., 2006), (Liu et al., 2014). In contrast to these microsurgical techniques, LACE has the advantageous capability of enzymatically removing the connective tissue, thereby reducing the risk of surgical nerve injury (Rydevik et al., 1985). The long term response of the nerve to collagenase and the ability to induce axonal sprouting remain to be investigated.

The main objective of this study was to test LACE and its feasibility to perform acute *in vivo* stimulation, recording and drug delivery on rat sciatic nerve. This study is the first demonstration of the LACE's potential to offer a new, drug delivery-based extraneural approach to peripheral nerve interfacing for developing hybrid bionic systems and bioelectronic medicines.

In future studies, we will design packaging for chronic LACE implantation including electrical and drug delivery components. We will then perform functional testing of LACE in chronic implantation conditions including nerve health and stability of the interface after delivery of collagenase to elucidate possible level of axonal inflammation and fibrosis. We will also evaluate the electrodes for cross-talk and impedance spectra to quantify leakage current, electrode performance, and wiring integrity for chronic electrophysiological recording and electrical stimulation experiments. We expect that these results will be one step closer to offering a solution for selective nerve stimulation and recording for biomedicine application.

Acknowledgements

This work was sponsored by the Defense Advanced Research Projects Agency (DARPA) BTO under the auspices of Drs. Doug Weber and Eric Van Gieson through the DARPA Contracts Management Office Cooperative Agreement HR0011-15-2-0006. C.L. was partially supported by the University of Southern California Provost Fellowship. The authors would like to thank Dr. Victor Pikov (Medipace), Mr. Jason Miranda (Galvani), and Dr. Srikanth Vasudevan (FDA) for their guidance, and Dr. Thai Truong, Peter Luu and the USC Translational Imaging Center for their imaging assistance.

References

Badia, J., Boretius, T., Andreu, D., Azevedo-Coste, C., Stieglitz, T., Navarro, X., 2011. Comparative analysis of transverse intrafascicular multichannel, longitudinal intrafascicular and multipolar cuff electrodes for the selective stimulation of nerve fascicles. J. Neural Eng. 8 (June 3), 036023. https://doi.org/10.1088/1741-2560/8/3/036023.

Banni, S., et al., 2012. Vagus nerve stimulation reduces body weight and fat mass in rats. PLoS One 7 (September 9), e44813. https://doi.org/10.1371/journal.pone.0044813.

Campagnola, P.J., Millard, A.C., Terasaki, M., Hoppe, P.E., Malone, C.J., Mohler, W.A., 2002. Three-dimensional high-resolution second-harmonic generation imaging of endogenous structural proteins in biological tissues. Biophys. J. 82 (January 1), 493–508. https://doi.org/10.1016/S0006-3495(02)75414-3.

Caparso, A.V., Durand, D.M., Mansour, J.M., 2009. A nerve cuff electrode for controlled reshaping of nerve geometry. J. Biomater. Appl. 24 (September 3), 247–273. https://doi.org/10.1177/0885328208097426.

Caravaca, A.S., et al., 2017. A novel flexible cuff-like microelectrode for dual purpose, acute and chronic electrical interfacing with the mouse cervical vagus nerve. J. Neural Eng. 14 (December 6), 066005. https://doi.org/10.1088/1741-2552/aa7a42.

Cobo, A.M., et al., 2019. Parylene-based cuff electrode with integrated microfluidics for peripheral nerve recording, stimulation, and drug delivery. J. Microelectromech. Syst. 28 (Febuary 1), 36–49. https://doi.org/10.1109/JMEMS.2018.2881908.

Cogan, S.F., 2008. Neural Stimulation and Recording Electrodes. Annu. Rev. Biomed. Eng. 10 (August 1), 275–309. https://doi.org/10.1146/annurev.bioeng.10.061807.160518.

del Valle, J., Navarro, X., 2013. Chapter Two - interfaces with the peripheral nerve for the control of neuroprostheses. In: In: Geuna, S., Perroteau, I., Tos, P., Battiston, B. (Eds.), International Review of Neurobiology, vol. 109. Academic Press, pp. 63–83.

Elyahoodayan, S., Larson, C., Meng, E., Song, D., 2018. Acute electrophysiological and

drug delivery tests of parylene cuff electrode with embedded microfluid channels. In: 43rd Neural Interfaces Conference. Minneapolis, MN.
Giagka, V., Serdijn, W.A., 2018. Realizing flexible bioelectronic medicines for accessing the peripheral nerves – technology considerations. Bioelectron. Med. 4 (December 1). https://doi.org/10.1186/s42234-018-0010-y.
Graczyk, E.L., Schiefer, M.A., Saal, H.P., Delhaye, B.P., Bensmaia, S.J., Tyler, D.J., 2016. The neural basis of perceived intensity in natural and artificial touch. Sci. Transl. Med. 8 (October (362)). https://doi.org/10.1126/scitranslmed.aaf5187. p. 362ra142.
Grill, W.M., Mortimer, J.T., 1996. Non-invasive measurement of the input-output properties of peripheral nerve stimulating electrodes. J. Neurosci. Methods 65 (March 1), 43–50. https://doi.org/10.1016/0165-0270(95)00143-3.
Guiraud, D., et al., 2016. Vagus nerve stimulation: state of the art of stimulation and recording strategies to address autonomic function neuromodulation. J. Neural Eng. 13 (August 4), 041002. https://doi.org/10.1088/1741-2560/13/4/041002.
Hoffer, J.A., Kallesøe, K., 2001. How to use nerve cuffs to stimulate, record or modulate neural activity. In: Moxon, K.A., Chapin, J.K. (Eds.), Neural Prostheses for Restoration of Sensory and Motor Function. CRC Press, pp. 139–175.
Huxley, A.F., Stämpeli, R., 1949. Evidence for saltatory conduction in peripheral myelinated nerve fibres. J. Physiol. 108 (May 3), 315–339. https://doi.org/10.1113/jphysiol.1949.sp004335.
Kang, X., Liu, J.-Q., Tian, H., Yang, B., Nuli, Y., Yang, C., 2015. Self-closed parylene cuff electrode for peripheral nerve recording. J. Microelectromech. Syst. 24 (April 2), 319–332. https://doi.org/10.1109/JMEMS.2014.2381634.
Koopman, F.A., et al., 2016. Vagus nerve stimulation inhibits cytokine production and attenuates disease severity in rheumatoid arthritis. Proc. Natl. Acad. Sci. 113 (July 29), 8284–8289. https://doi.org/10.1073/pnas.1605635113.
Larson, C.E., Meng, E., 2019. A review for the peripheral nerve interface designer. J. Neurosci. Methods 108523. https://doi.org/10.1016/j.jneumeth.2019.108523. November.
Lawrence, S.M., Larsen, J.O., Horch, K.W., Riso, R., Sinkjaer, T., 2002. Long-term biocompatibility of implanted polymer-based intrafascicular electrodes: implanted Polymer-Based Intrafascicular Electrodes. J. Biomed. Mater. Res. 63 (5), 501–506. https://doi.org/10.1002/jbm.10303.
Leventhal, D.K., Durand, D.M., 2003. Subfascicle stimulation selectivity with the flat interface nerve electrode. Ann. Biomed. Eng. 31 (June 6), 643–652. https://doi.org/10.1114/1.1569266.
Leventhal, D.K., Cohen, M., Durand, D.M., 2006. Chronic histological effects of the flat interface nerve electrode. J. Neural Eng. 3 (June 2), 102–113. https://doi.org/10.1088/1741-2560/3/2/004.
Liang, D.H., Kovacs, G.T.A., Storment, C.W., White, R.L., 1991. A method for evaluating the selectivity of electrodes implanted for nerve simulation. IEEE Trans. Biomed. Eng. 38 (May 5), 443–449. https://doi.org/10.1109/10.81563.
Liu, H.-F., Chen, Z.-G., Fang, T.-L., Arnold, P., Lineaweaver, W.C., Zhang, J., 2014. Changes of the donor nerve in end-to-side neurorrhaphies with epineurial window and partial neurectomy: a long-term evaluation in the rat model. Microsurgery 34 (Febuary 2), 136–144. https://doi.org/10.1002/micr.22167.
Lloyd, Hodgkin Alan, Hugh, Rushton William Albert, Douglas, Adrian Edgar, 1946. The electrical constants of a crustacean nerve fibre. Proc. R. Soc. Lond. Ser. B - Biol. Sci. 133 (December 873), 444–479. https://doi.org/10.1098/rspb.1946.0024.
Loeb, G.E., Peck, R.A., 1996. Cuff electrodes for chronic stimulation and recording of peripheral nerve activity. J. Neurosci. Methods 64 (January 1), 95–103. https://doi.org/10.1016/0165-0270(95)00123-9.
Marks, W.B., Loeb, G.E., 1976. Action currents, internodal potentials, and extracellular records of myelinated mammalian nerve fibers derived from node potentials. Biophys. J. 16 (June 6), 655–668. https://doi.org/10.1016/S0006-3495(76)85719-0.
Maynard, E.M., Nordhausen, C.T., Normann, R.A., 1997. The utah intracortical electrode array: a recording structure for potential brain-computer interfaces. Electroencephalogr. Clin. Neurophysiol. 102 (March 3), 228–239. https://doi.org/10.1016/S0013-4694(96)95176-0.
McCallister, W.V., Tang, P., Smith, J., Trumble, T.E., 2001. Axonal regeneration stimulated by the combination of nerve growth factor and ciliary neurotrophic factor in an end-to-side model. J. Hand Surg. 26 (May 3), 478–488. https://doi.org/10.1053/jhsu.2001.24148.
Navarro, X., Krueger, T.B., Lago, N., Micera, S., Stieglitz, T., Dario, P., 2005. A critical review of interfaces with the peripheral nervous system for the control of neuroprostheses and hybrid bionic systems. J. Peripher. Nerv. Syst. 10 (September 3), 229–258. https://doi.org/10.1111/j.1085-9489.2005.10303.x.
Picaza, J.A., Hunter, S.E., Cannon, B.W., 1977. Pain suppression by peripheral nerve stimulation. Stereotact. Funct. Neurosurg. 40, 223–234. https://doi.org/10.1159/000102446. no. 2–4.
Plachta, D.T.T., et al., 2014. Blood pressure control with selective vagal nerve stimulation and minimal side effects. J. Neural Eng. 11 (June 3), 036011. https://doi.org/10.1088/1741-2560/11/3/036011.
Rodríguez, F.J., et al., 2000. Polyimide cuff electrodes for peripheral nerve stimulation. J. Neurosci. Methods 98 (June 2), 105–118. https://doi.org/10.1016/S0165-0270(00)00192-8.
Russell, C., Roche, A.D., Chakrabarty, S., 2019. Peripheral nerve bionic interface: a review of electrodes. Int. J. Intell. Robot. Appl. 3 (March 1), 11–18. https://doi.org/10.1007/s41315-019-00086-3.
Rydevik, B., Brown, M., Ehira, T., Nordborg, C., 1985. Effects of collagenase on nerve tissue. An experimental study on acute and long-term effects in rabbits. Spine 10 (6), 562–566.
Šámal, F., Haninec, P., Raška, O., Dubový, P., 2006. Quantitative assessment of the ability of collateral sprouting of the motor and primary sensory neurons after the end-to-side neurorrhaphy of the rat musculocutaneous nerve with the ulnar nerve. Ann. Anat. 188 (July 4), 337–344. https://doi.org/10.1016/j.aanat.2006.01.017.
Schiefer, M.A., Polasek, K.H., Triolo, R.J., Pinault, G.C.J., Tyler, D.J., 2010. Selective stimulation of the human femoral nerve with a flat interface nerve electrode. J. Neural Eng. 7 (April 2), 026006. https://doi.org/10.1088/1741-2560/7/2/026006.
Schultz, A.E., Kuiken, T.A., 2011. Neural interfaces for control of upper limb prostheses: the state of the art and future possibilities. PMR 3 (January 1), 55–67. https://doi.org/10.1016/j.pmrj.2010.06.016.
Sinclair, E.B., Andarawis-Puri, N., Ros, S.J., Laudier, D.M., Jepsen, K.J., Hausman, M.R., 2012. Relating applied strain to the type and severity of structural damage in the rat median nerve using second harmonic generation microscopy. Muscle Nerve 46 (December 6), 895–898. https://doi.org/10.1002/mus.23443.
Sun, F.T., Morrell, M.J., 2014. Closed-loop neurostimulation: the clinical experience. Neurotherapeutics 11 (July 3), 553–563. https://doi.org/10.1007/s13311-014-0280-3.
Tan, D.W., Schiefer, M.A., Keith, M.W., Anderson, J.R., Tyler, D.J., 2015. Stability and selectivity of a chronic, multi-contact cuff electrode for sensory stimulation in human amputees. J. Neural Eng. 12 (April 2), 026002. https://doi.org/10.1088/1741-2560/12/2/026002.
Vedantham, V., Cannon, S.C., 1999. The position of the fast-inactivation gate during lidocaine block of voltage-gated Na^+ channels. J. Gen. Physiol. 113 (January 1), 7–16. https://doi.org/10.1085/jgp.113.1.7.
Vijayaraghavan, S., Huq, R., Hausman, M.R., 2014. Methods of peripheral nerve tissue preparation for second harmonic generation imaging of collagen fibers. Methods 66 (2), 246–255. https://doi.org/10.1016/j.ymeth.2013.08.012.
Xue, N., et al., 2015. Polymeric C-shaped cuff electrode for recording of peripheral nerve signal. Sens. Actuators B Chem. 210, 640–648. https://doi.org/10.1016/j.snb.2015.01.006. April.
Yu, H., Xiong, W., Zhang, H., Wang, W., Li, Z., 2014. A Cable-tie-type Parylene Cuff Electrode for Peripheral Nerve Interfaces. pp. 9–12. https://doi.org/10.1109/MEMSYS.2014.6765560.
Zabara, J., 1985. Peripheral control of hypersynchronous discharge in epilepsy," *Electroencephalogr.* Clin. Neurophysiol. 61 (September 3), S162. https://doi.org/10.1016/0013-4694(85)90626-1.
Zoumi, A., Yeh, A., Tromberg, B.J., 2002. Imaging cells and extracellular matrix in vivo by using second-harmonic generation and two-photon excited fluorescence. Proc. Natl. Acad. Sci. 99 (17), 11014–11019. https://doi.org/10.1073/pnas.172368799.